INTERNATIONAL JOURNAL FOR NUMERICAL METHODS IN FLUIDS, VOL. 18, 803–819 (1994)

A FINITE VOLUME SCHEME FOR TWO-PHASE COMPRESSIBLE FLOWS

R. SAUREL

IUSTI-CNRS 1168 Ecoulements Diphasiques et Réactifs, Case 321, Av. Escadrille, Normandie-Niemen, F-13397 Marseille Cedex 20, France

A. FORESTIER

CEN Saclay, DRN/DMT/SEMT/VIBR, F-91191 Gif-sur-Yvette, France and Université EVE, Centre CEMIF, Bd. des Coquibus, F-91025 Evry Ville Nouvelle, France

AND

D. VEYRET AND J.-C. LORAUD

IUSTI-CNRS 1168 Ecoulements Diphasiques et Réactifs, Case 321, Av. Escadrille, Normandie-Niemen, F-13397 Marseille Cedex 20, France

SUMMARY

In gas–particle two-phase flows, when the concentration of the dispersed phase is low, certain assumptions may be made which simplify considerably the equations one has to solve. The gas and particle flows are then linked only via the interaction terms. One may therefore uncouple the full system of equations into two subsystems: one for the gas phase, whose homogeneous part reduces to the Euler equations; and a second system for the particle motion, whose homogeneous part is a degenerate hyperbolic system. The equations governing the gas phase flow may be solved using a high-resolution scheme, while the equations describing the motion of the dispersed phase are treated by a donor–cell method using the solution of a particular Riemann problem. Coupling is then achieved via the right-hand-side terms. To illustrate the capabilities of the proposed method, results are presented for a case specially chosen from among the most difficult to handle, since it involves certain geometrical difficulties, the treatment of regions in which particles are absent and the capturing of particle fronts.

KEY WORDS Two-phase Riemann solver TVD scheme Laminar spray

1. INTRODUCTION

Two-phase flows are encountered in numerous industrial applications ranging from internal combustion engines to space vehicle propulsion and even in nuclear energy processes. These flows may take various forms depending upon the actual state.[1] Among these types, one is commonly known as the dispersed phase flow: one of the phases is dispersed within the other and most often carried along with it. It is this particular type of flow we shall refer to in the following.

It is essential to make a distinction between flows in which the gas phase is heavily loaded with particles and those in which the particle content is diluted. Although no fundamental difference arises in the physical approach to these two types, the assumptions that one may be led to adopt in either of these cases might change the mathematical nature of the equations to be solved and subsequently might impose the choice of the numerical method to be employed.

CCC 0271–2091/94/090803–17

Received November 1992
Revised October 1993

In most numerical simulations of gas–particle two-phase flows available in the literature, the 'two-fluid' model is commonly retained. In this model the gas and dispersed phases are treated as distinct continuous media, while momentum and energy exchanges take place across the particle surface involving the viscosity and thermal conductivity. In the case of a heavily laden flow the basic equations in the two-fluid model are as follows.[2]

Conservation of mass

$$\frac{\partial}{\partial t}[\alpha_g \rho_g] + \frac{\partial}{\partial x}[\alpha_g \rho_g u_g] = [\Gamma]_g^i, \tag{1a}$$

$$\frac{\partial}{\partial t}[\alpha_s \rho_s] + \frac{\partial}{\partial x}[\alpha_s \rho_s u_s] = -[\Gamma]_g^i, \tag{1b}$$

where ρ_k and u_k are the density and the x-component of velocity respectively for phase k and α_g is the void fraction ($\alpha_g = 1 - \alpha_s$).

Conservation of momentum

$$\frac{\partial}{\partial t}[\alpha_g \rho_g u_g] + \frac{\partial}{\partial x}[\alpha_g \rho_g u_g^2] + \frac{\partial}{\partial x}[\alpha_g P_g] = P_g \frac{\partial \alpha_g}{\partial x} + [\Gamma_V]_g^i + [F_d]_g^i, \tag{2a}$$

$$\frac{\partial}{\partial t}[\alpha_s \rho_s u_s] + \frac{\partial}{\partial x}[\alpha_s \rho_s u_s^2] + \frac{\partial}{\partial x}[\alpha_s P_s] = -P_g \frac{\partial \alpha_g}{\partial x} - [\Gamma_V]_g^i - [F_d]_g^i, \tag{2b}$$

where P_k is the pressure of phase k.

Conservation of energy—first law of thermodynamics

$$\frac{\partial}{\partial t}[\alpha_g \rho_g e_g] + \frac{\partial}{\partial x}[\alpha_g \rho_g e_g u_g] + \frac{\partial}{\partial x}[\alpha_g P_g u_g] = -P_g \frac{\partial \alpha_g}{\partial t} + \Gamma_g^i E_{chem} + [\Gamma_{EC}]_g^i + [Q]_g^i + [F_d]_g^i u_s, \tag{3a}$$

$$\frac{\partial}{\partial t}[\alpha_s \rho_s e_s] + \frac{\partial}{\partial x}[\alpha_s \rho_s e_s u_s] + \frac{\partial}{\partial x}[\alpha_s P_s u_s] = P_g \frac{\partial \alpha_g}{\partial t} - [\Gamma_{EC}]_g^i - [Q]_g^i - [F_d]_g^i u_s, \tag{3b}$$

where e_k is the total energy per unit mass of phase k.

Evolution of the real density of the dispersed phase. The inequality relation for the entropy suggests a relation for the dynamic compaction allowing one to take into account the compressibility of each phase:

$$\frac{\partial}{\partial t}[\rho_s] + \frac{\partial}{\partial x}[\rho_s u_s] = \frac{\alpha_g \alpha_s}{\mu_c}[P_s - P_g - R_p], \tag{4}$$

where R_p is the interparticle stress tensor and μ_c is the dynamic compaction viscosity.

In these equations the right-hand sides are coupling terms: mass transfer in equations (1a) and (1b); momentum transfer induced by mass transfer and drag forces in equations (2a) and (2b); and energy transfer induced by mass transfer, convective heat flux and work of drag forces in equations (3a) and (3b). We shall not dwell on these terms; their expressions may be found in References 2–4.

A mathematical analysis of this system of equations carried out by Embid and Baer[5] has revealed that it admits a number of distinct characteristic directions and therefore the system is strictly hyperbolic under certain conditions. Hyperbolicity is due to the existence of a pressure disequilibrium between the phases during compaction processes; this is taken into account by the introduction of an intergranular stress tensor representing the forces exerted between the particles. Owing to its hyperbolic aspect, the system may (in principle) be solved by classical numerical methods already in common use in gas-dynamics, among which the most popular are the finite difference scheme of MacCormack[6] and the finite volume formulations of Van Leer[7] and Roe.[8] This system has been solved for the first time by Baer and Nunziato[2] using the flux-corrected transport method due to Book *et al.*[9] (finite differences). Soon afterwards Toro[10] proposed a Godunov-type method[11] (finite volume) in which a Riemann problem was solved for the subsystem of the particle phase in a slightly simplified case.

Flows of heavily laden fluids with particles must be contrasted with highly diluted ones. For the latter case a number of simplifying assumptions may be made, mainly upon the volume occupied by the particles and its implication in the pressure terms.[12] One is then led to solving the following system, which is formally simpler and widely used:[13–17]

$$\begin{aligned}
&\frac{\partial \rho_g}{\partial t} + \frac{\partial \rho_g u_g}{\partial x} = 0,\\
&\frac{\partial \rho_g u_g}{\partial t} + \frac{\partial (\rho_g u_g^2 + P)}{\partial x} = [F_d]_g^i,\\
&\frac{\partial \rho_g e_g}{\partial t} + \frac{\partial u_g(\rho_g e_g + P)}{\partial x} = [F_d]_g^i u_s;
\end{aligned} \tag{5}$$

$$\begin{aligned}
&\frac{\partial \rho_s}{\partial t} + \frac{\partial \rho_s u_s}{\partial x} = 0,\\
&\frac{\partial \rho_s u_s}{\partial t} + \frac{\partial \rho_s u_s^2}{\partial x} = -[F_d]_g^i,\\
&\frac{\partial \rho_s e_s}{\partial t} + \frac{\partial \rho_s u_s e_s}{\partial x} = -[F_d]_g^i u_s.
\end{aligned} \tag{6}$$

System (5) is readily identified as the Euler equations; one should also remark that systems (5) and (6) are coupled only by the phase interaction terms, the void fraction being absent (compare with system (1)–(3)). The homogeneous left-hand parts of systems (5) and (6) being uncoupled, they may therefore be solved independently. One then recovers for system (5) the three well-known real characteristic directions $u + a$, $u - a$ and u (a being the sound speed); this ensures the hyperbolic nature of the system and allows a relatively easy resolution with the help, for example, of some high-resolution scheme.[7,8] System (6), on the other hand, admits only a single characteristic direction u_s. It can be shown that this system is hyperbolic degenerate and may have multivalued solutions. We shall come back to this difficulty in the next section and propose an efficient method for solving the system of equations (5) and (6) generalized to the two-dimensional case.

When studying highly diluted flows, other formulations are available that solve for a distribution of particle size and velocities.[18,19] In this formulation a similar system of equations to (5) and (6) is first obtained. In this approach the gas-phase equations are commonly solved by

a Eulerian method while the particle equations are solved by a Lagrangian method. This procedure has been widely used.[13,20] When the flow contains particles of different sizes or with a velocity distribution which cannot be considered as a barycentric velocity, the Liouville–Boltzmann equation can be added to the formulation. This formulation is sometimes called the spray formulation equations.[18] The solution of this complete formulation—gas phase equations, Lagrangian particle phase equations and Liouville–Boltzmann equation—can be obtained by the method developed by Dukowicz.[21] This formulation gives excellent results and is of particular interest when solving complex flow configurations (e.g. particle vortices). When the flow configuration is not so complex, which is the case for many industrial applications where particles are generally accelerated continuously from the injector to the exit, the method presented herein can be sufficiently accurate. In addition, in many industrial applications the difficulty is related to the geometry, which is why we propose a numerical method suitable for unstructured meshes. The present method is a pure Eulerian formulation and can produce reliable results in a very short computational time. In contrast, using a Lagrangian scheme for the particle phase is expensive when the gas equations are solved on an unstructured mesh. The expensiveness comes from the research of the neighbouring cells of gas around a Lagrangian location of a group of particles, where interpolations are to be performed in order to couple the two systems.

We must recall that between these two extreme cases of heavily laden and highly diluted media there also exists the case of flows moderately laden with particles. The system of equations describing such flows is a non-conservative one. Sainsaulieu and Raviart[22] have carried out a mathematical analysis of the type of these equations. Assuming that a difference in pressure exists between the gas and liquid phases owing to the surface tension, one obtains a strictly hyperbolic system. The same authors have proposed a numerical approach extending Roe's scheme; however, this procedure does not seem to be readily extended to gas–solid particle flows.

The next section will be devoted to (i) a mathematical study of the system (5), (6) extended to the two-dimensional case and (ii) the development of a finite volume formulation allowing the treatment of diluted two-phase flows in complex geometries. We shall then give some comparison with existing schemes to provide validation of the current scheme and afterwards other results illustrating the capabilities of the method. We conclude by discussing the research perspectives in this domain.

2. NUMERICAL SCHEME

The equations of the two-fluid model applied to the case of diluted two-phase flows are written as follows in two-dimensional Cartesian co-ordinates:

$$\begin{aligned}
&\frac{\partial \rho_g}{\partial t} + \frac{\partial \rho_g u_g}{\partial x} + \frac{\partial \rho_g v_g}{\partial y} = 0,\\
&\frac{\partial \rho_g u_g}{\partial t} + \frac{\partial (\rho_g u_g^2 + P)}{\partial x} + \frac{\partial (\rho_g u_g v_g)}{\partial y} = [F_{d_x}]_g^i,\\
&\frac{\partial \rho_g v_g}{\partial t} + \frac{\partial (\rho_g u_g v_g)}{\partial x} + \frac{\partial (\rho_g v_g^2 + P)}{\partial y} = [F_{d_y}]_g^i,\\
&\frac{\partial \rho_g e_g}{\partial t} + \frac{\partial u_g (\rho_g e_g + P)}{\partial x} + \frac{\partial v_g (\rho_g e_g + P)}{\partial y} = [F_{d_x}]_g^i u_s + [F_{d_y}]_g^i v_s;
\end{aligned} \tag{7}$$

$$\frac{\partial \rho_s}{\partial t} + \frac{\partial \rho_s u_s}{\partial x} + \frac{\partial \rho_s v_s}{\partial y} = 0,$$

$$\frac{\partial \rho_s u_s}{\partial t} + \frac{\partial \rho_s u_s^2}{\partial x} + \frac{\partial \rho_s u_s v_s}{\partial y} = -[F_{d_x}]_g^i, \tag{8}$$

$$\frac{\partial \rho_s v_s}{\partial t} + \frac{\partial \rho_s u_s v_s}{\partial x} + \frac{\partial \rho_s v_s^2}{\partial y} = -[F_{d_y}]_g^i.$$

We notice that in order to simplify matters, the particles are assumed to exchange neither mass nor energy. The gas–particle interactions are therefore assumed to be due only to the drag forces. We point out, however, that in principle there is no difficulty in also taking into account the mass and energy transfers.

In addition some assumptions are formulated.

1. The volume occupied by the particles is negligible.
2. The particles are spherical and monodisperse.
3. Collisions, coalescence and break-up are not considered.
4. Turbulence is not considered.
5. The particle velocity is a barycentric velocity, which means that in each cell all particles are assumed to have an average velocity.

If the behaviour of different sizes of particles is needed, one has to solve as many systems (8) as there are sizes of particles. This is a limitation of this formulation.

Systems (7) and (8) being uncoupled, the homogeneous problems can be solved separately for the gas and particle systems. To summarize, the following procedure results.

1. Solve the homogeneous problem for the gas motion.
2. Solve the homogeneous problem for the particles.
3. Couple the two systems via the interaction terms.

2.1. Solution of the homogeneous system for the gas flow

The homogeneous part of system (6) is actually the Euler equation and may be written in the vector form

$$\frac{\partial U}{\partial t} + \frac{\partial F_1}{\partial x} + \frac{\partial F_2}{\partial y} = 0. \tag{9}$$

The following method is an extension of Van Leer's scheme for unstructured meshes due to Forestier.[23] Within an unstructured mesh define a cell T_j in which the solution is assumed to be piecewise linear; this solution will thus be determined by a certain mean value U_j^n and by two slopes, d_j^n in the x-direction and δ_j^n in the y-direction. Define also by $I(j)$ ($j = 1$–4) all the neighbouring cells of T_j, and denote by δT_j the boundary of T_j (Figure 1).

Let ω_j and ω_{j1} be the centres of gravity of cells T_j and T_{j1} with co-ordinates $(x_{\omega_j}, y_{\omega_j})$ and $(x_{\omega_{j1}}, y_{\omega_{j1}})$ respectively.

(a) The first (predictor) step consists of computing the values of $U_{\delta T_j}^{n+1/2}$ viewed from the contour δT_j. As an example take $\delta T_j \cap \delta T_{j1}$. First

$$U_{\delta T_j \cap \delta T_{j1}}^n = U_j^n + \tfrac{1}{2} d_j^n (x_{\omega_j} - x_{\omega_{j1}}) + \tfrac{1}{2} \delta_j^n (y_{\omega_j} - y_{\omega_{j1}}).$$

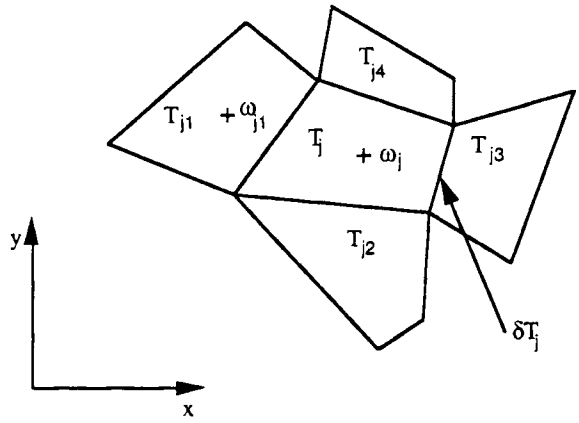

Figure 1. Elements of an unstructured mesh

Then

$$U^{n+1/2}_{\delta T_j \cap \delta T_{j1}} = U^{n}_{\delta T_j \cap \delta T_{j1}} + \frac{\Delta t}{2}\left(\frac{\partial U}{\partial t}\right)^{n}_{\delta T_j \cap \delta T_{j1}}.$$

However,

$$\frac{\partial U}{\partial t} + \frac{\partial F_1}{\partial U}\frac{\partial U}{\partial x} + \frac{\partial F_2}{\partial U}\frac{\partial U}{\partial y} = 0.$$

Thus

$$U^{n+1/2}_{\delta T_j \cap \delta T_{j1}} = U^{n}_{j} + \tfrac{1}{2} d^{n}_{j}(x_{\omega_j} - x_{\omega_{j1}}) + \tfrac{1}{2}\delta^{n}_{j}(y_{\omega_j} - y_{\omega_{j1}}) - \frac{\Delta t}{2}\frac{\partial F_1(U^{n}_{j})}{\partial U} d^{n}_{j} - \frac{\Delta t}{2}\frac{\partial F_2(U^{n}_{j})}{\partial U}\delta^{n}_{j}.$$

(b) We now need to write down the fluxes of the various variables which cross the interface $\delta T_j \cap \delta T_{j1}$ along the normal to this line; we are then led to a one-dimensional Riemann problem.

Denote by $\vec{n}$ the outward-pointing normal to the line $\delta T_j \cap \delta T_{j1}$; define also the vector $V_{\vec{n}}(\vec{u}) = (\rho, \rho\vec{u}\vec{n}, \rho E)^T$ associated with the vector $U = (\rho, \rho u, \rho v, \rho E)^T$, where $\vec{u} = (u, v)^T$. The vector $V_{\vec{n}}(\vec{u})$, which will allow us to compute the fluxes along the normal direction, results as the solution to the Riemann problem set at the interface between the two cells:

$$V^{n+1/2}_{\delta T_j \cap \delta T_{j1}} = W[0;\ V_{\vec{n}\delta T_j \cap \delta T_{j1}}(U^{n+1/2}_{\delta T_j \cap \delta T_{j1}});\ V_{\vec{n},\delta T_j \cap \delta T_{j1}}(U^{n+1/2}_{\delta T_{j1} \cap \delta T_j})].$$

(c) One may now apply the conservation law

$$\frac{U^{n+1}_{j} - U^{n}_{j}}{\Delta t} + \frac{1}{S_{T_j}}\sum_{k=1}^{I(j)}\left[\int_{\delta T_j \cap \delta T_{jk}} F_1(V^{n+1/2}_{\delta T_j \cap \delta T_{jk}}) n_1 \, d\sigma + \int_{\delta T_j \cap \delta T_{jk}} F_2(V^{n+1/2}_{\delta T_j \cap \delta T_{jk}}) n_2 \, d\sigma\right] = 0,$$

where $\vec{n} = (n_1, n_2)$.

It is noticed that $F_i(V^{n+1/2}_{\delta T_j \cap \delta T_{jk}})$ is computed at the middle of each face and is assumed constant along each segment. Denoting by n_i one of the components of the unit normal to a segment, one may then write

$$\int_{\delta T_j \cap \delta T_{jk}} F_i(V^{n+1/2}_{\delta T_j \cap \delta T_{jk}}) n_i \, d\sigma = F_i(V^{n+1/2}_{\delta T_j \cap \delta T_{jk}}) n^*_{i, \delta T_j \cap \delta T_{jk}},$$

where n_i^* is one of the components of the non-unit normal to the face $\delta T_j \cap \delta T_{jk}$. One then obtains

$$\frac{U_j^{n+1} - U_j^n}{\Delta t} + \frac{1}{S_{T_j}} \sum_{k=1}^{I(j)} [F_1(V^{n+1/2}_{\delta T_j \cap \delta T_{jk}}) n^*_{1, \delta T_j \cap \delta T_{jk}} + F_2(V^{n+1/2}_{\delta T_j \cap \delta T_{jk}}) n^*_{2, \delta T_j \cap \delta T_{jk}}] = 0.$$

(d) We only need to compute the slopes of conservative variables on each element. For this purpose one applies the total-variation-diminishing (TVD) procedure: if

$$\frac{U_j^{n+1} - U_k^n}{x_{\omega_j} - x_{\omega_k}} \quad \text{for } k = j1, \ldots, j4$$

are of the same sign, then

$$d_j^{n+1} = \operatorname{sign}\left(\frac{U_j^{n+1} - U_{j1}^n}{x_{\omega_j} - x_{\omega_{j1}}}\right) \min_{k=j1,\ldots,j4} \left| \frac{U_1^{n+1} - U_k^n}{x_{\omega_j} - x_{\omega_k}} \right|;$$

otherwise

$$d_j^{n+1} = 0.$$

This summarizes the minmod flux function. The procedure is the same for the slopes along the y-direction.

2.2. *Solution of the homogeneous problem for the particle motion*

Before dwelling on the solution procedure for the homogeneous part of system (8), we must make certain preliminary remarks. These equations may be written as

$$\begin{aligned} &\frac{\partial \rho_s}{\partial t} + \frac{\partial \rho_s u_s}{\partial x} + \frac{\partial \rho_s v_s}{\partial y} = 0, \\ &\frac{\partial \rho_s u_s}{\partial t} + \frac{\partial \rho_s u_s^2}{\partial x} + \frac{\partial \rho_s u_s v_s}{\partial y} = 0, \\ &\frac{\partial \rho_s v_s}{\partial t} + \frac{\partial \rho_s u_s v_s}{\partial x} + \frac{\partial \rho_s v_s^2}{\partial y} = 0. \end{aligned} \tag{10}$$

By combining the equation of mass conservation with the momentum equation, one obtains the system

$$\begin{aligned} &\frac{\partial \rho_s}{\partial t} + \frac{\partial \rho_s u_s}{\partial x} + \frac{\partial \rho_s v_s}{\partial y} = 0, \\ &\frac{\partial u_s}{\partial t} + u_s \frac{\partial u_s}{\partial x} + v_s \frac{\partial u_s}{\partial y} = 0, \\ &\frac{\partial v_s}{\partial t} + u_s \frac{\partial v_s}{\partial x} + v_s \frac{\partial v_s}{\partial y} = 0, \end{aligned} \tag{11}$$

where the equations of motion have been replaced by the two-dimensional equivalent of the Burgers equations. Obviously in the 1D case the relevant equations would be

$$\frac{\partial \rho_s}{\partial t} + \frac{\partial \rho_s u_s}{\partial x} = 0, \tag{12}$$

$$\frac{\partial u_s}{\partial t} + u_s \frac{\partial u_s}{\partial x} = 0. \tag{13}$$

This type of system has been studied by Miura and Glass[16] and recently by Forestier and Le Floch.[24] Equation (13) (the Burgers equation) may be solved separately since it is independent of equation (12). Now the Burgers equation admits shocks as solutions, whereas by applying the Hugoniot relations to system (10) (or to its 1D equivalent), one finds that in our case shocks cannot subsist.[24] One must conclude that the equations for the particle motion written in the form (10) fail to provide a physically realistic solution in the vicinity of shocks. In addition, solving the Burgers equations separately provides a unique value for the velocity, instead of two values as is possible for the multivaluated system (10). Several ways out of this impasse can be envisaged. The first consists of solving equation (10) in such a manner as to avoid the formation of a shock, as proposed by Miura and Glass,[16] but then extension to the 2D case becomes difficult. Another approach would be to solve equations (10) by a Lagrangian method, as done by Ishii *et al.*[13] and Sommerfeld;[20] the trouble then arises from the difficulty in following the particles through a non-structured grid. As mentioned previously, in order to couple the gas and particle systems, one has to find the neighbouring cells around the location of each group of particles and then make interpolations. This operation is difficult and expensive in term of CPU time.

The most appealing procedure would seem to be to solve our equations in the form (10), since this system does not admit shocks. However, as pointed out above, this system possesses a single characteristic direction u_s (and v_s for the fluxes along y). Such a degenerate hyperbolic system cannot therefore be treated by the traditional methods of gas dynamics, which were established for strictly hyperbolic systems. In addition, because of the one-directional propagation of information, the system has to be solved by an upwind scheme. Among the formulations developed for gas dynamic applications, one particular scheme seems to possess the required features, namely the donor–cell scheme. This was left out owing to its poor performance at shock capturing, but in our present case shocks are absent. The solution obtained by the donor–cell scheme will have the additional advantage of verifying the Riemann problem evaluated at the interfaces (or intercells); therefore it is appropriate to envisage the Riemann problem for a multivalued system such as equations (10).

2.2.1. Solution of the Riemann problem for the equations of particle motion. Let us consider the one-dimensional case and assume that all magnitudes within the cells are piecewise constant. Denote by u the velocity and by ρ the apparent particle density; subscripts 'r' and 'l' relate to the right- and left-side states respectively, while superscript '*' marks the state retained at the interface of two cells.

(a) Expansion: $u_l < u_r$

(a1) $u_l > 0$ and $u_r > 0$ (Figure 2).

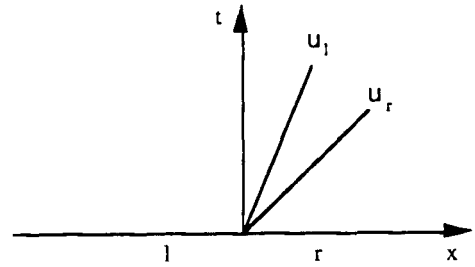

Figure 2. First configuration for the Riemann problem

The solution for this case is $\rho^* = \rho_l$, $u^* = u_l$.

(a2) $u_l < 0$ and $u_r > 0$ (Figure 3).

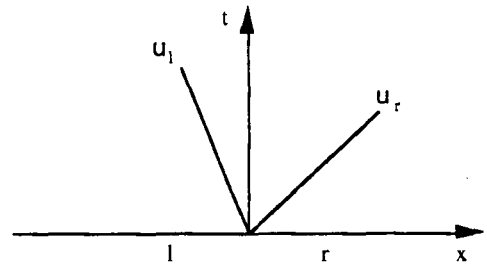

Figure 3. Second configuration for the Riemann problem

The solution for this case is $\rho^* = 0$. When a particle bed is set in motion simultaneously in two opposite directions, no particles are left at the interface (i.e. a particle void is produced).

(a3) $u_l < 0$ and $u_r < 0$ (Figure 4).

This case is symmetric with (a1), i.e. $\rho^* = \rho_r$, $u^* = u_r$.

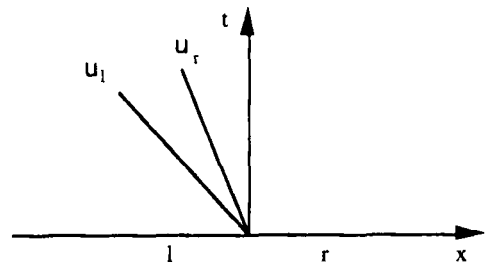

Figure 4. Third configuration for the Riemann problem

(b) Compression: $u_l > u_r$

(b1) $u_l > 0$ and $u_r > 0$ (Figure 5).

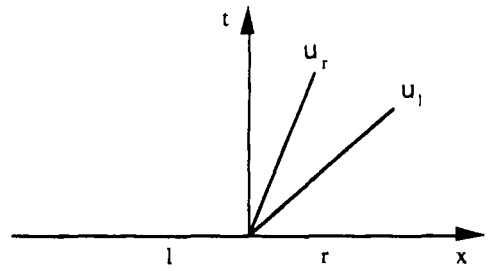

Figure 5. Fourth configuration for the Riemann problem

For this case the solution is $\rho^* = \rho_l$, $u^* = u_l$.
(b2) $u_l > 0$ and $u_r < 0$ (Figure 6).
The solution in this case is $\rho^* = \rho_l + \rho_r$, $(\rho u)^* = \rho_l u_l + \rho_r u_r$; therefore

$$u^* = (\rho_l u_l + \rho_r u_r)/(\rho_l + \rho_r).$$

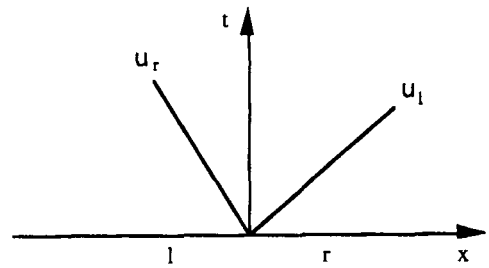

Figure 6. Fifth configuration for the Riemann problem

When two particle beds approach from opposite directions, they coalesce (since we have assumed that there does not exist any particle–particle interaction). The resulting concentration rate is the sum of the two rates (left and right); the flow rate is the algebraic sum of the two flow rates, thus yielding the velocity.

(b3) $u_l < 0$ and $u_r > 0$ (Figure 7).
This case is symmetric with (b1), i.e. $\rho^* = \rho_r$, $u^* = u_r$.

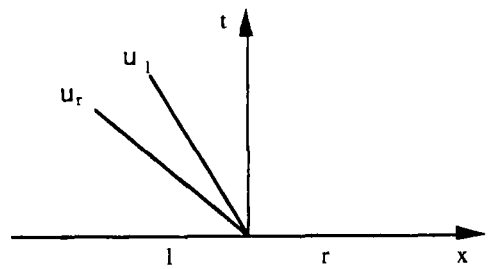

Figure 7. Sixth configuration for the Riemann problem

2.2.2. The donor–cell scheme in unstructured meshes. After writing system (8) in the vector form

$$\frac{\partial V}{\partial t} + \frac{\partial G_1}{\partial x} + \frac{\partial G_2}{\partial y} = 0$$

and making use of the notation introduced above, the donor–cell formulation for an unstructured mesh can be written as

$$\frac{V_j^{n+1} - V_j^n}{\Delta t} + \frac{1}{S_{T_j}} \sum_{k=1}^{I(j)} [G_1(\bar{V}) n^*_{1,\delta T_j \cap \delta T_{jk}} + G_2(\bar{V}) n^*_{2,\delta T_j \cap \delta T_{jk}}] = 0,$$

with the notation $\bar{V}$ meaning one of the six solutions of the Riemann problem.

This formulation presents a very important disadvantage. In fact, this balance equation over the control volume implies losing the history of each particle family. We have hereby introduced the important notion of particle family: this is characterized by its size (particle radius), density, momentum, energy or more generally its history. Why is losing the history of a particle important? Consider for example two jets of particles moving in opposite directions as shown in Figure 6. This is the extreme case of particle compression as defined above. When the conservation law is applied, we find as expected an increase in density, but the resulting momentum is an average momentum. If collisions are negligible because the medium is highly diluted, physically the two jets cross each other instead of having an average velocity. In summary, the conservation law applied in the donor–cell scheme is not compatible with a multivaled system where two velocities can exist at a given location. In contrast, if the resolution method was Lagrangian, with an independent following of each particle, the problem would be readily solved. For this reason the range of validity of Dukowicz's method[21] is larger than that of the present one. However, if we look at the significance of the particle Riemann problem and at the physical cases one has to treat most commonly, our method can constitute an interesting alternative to Dukowicz's method. Recall that among the six cases of the Riemann problem, three are related to expansions and the other three to compressions.

In the case of expansion zones any control volume contains particles with the same history, the only effect of an expansion being to pull the particles apart. Expansions correspond to numerous physical cases encountered in industrial applications. When particles are injected through an orifice, they are generally accelerated continuously to the exit by the gas flow. Compressions occur for example when faster particles reach the same control volume as slower particles. This kind of situation occurs in complex flows (e.g. particle vortices) and always when treating a particle–wall interaction or a symmetry axis. In practice, when the flow is very complex, one must resort to a Lagrangian formulation. However, when compressions occur only in the treatment of boundary conditions or in a limited number of regions of the particle flow, our method remains attractive. For example, for the treatment of a symmetry axis one has simply to introduce a second family of particles characterized by a new set of equations. Now one has to solve

$$\frac{\partial \rho_g}{\partial t} + \frac{\partial \rho_g u_g}{\partial x} + \frac{\partial \rho_g v_g}{\partial y} = 0,$$

$$\frac{\partial \rho_g u_g}{\partial t} + \frac{\partial (\rho_g u_g^2 + P)}{\partial x} + \frac{\partial (\rho_g u_g v_g)}{\partial y} = [F d_{x1}]_g^i + [F d_{x2}]_g^i,$$

$$\frac{\partial \rho_g v_g}{\partial t} + \frac{\partial (\rho_g u_g v_g)}{\partial x} + \frac{\partial (\rho_g v_g^2 + P)}{\partial y} = [Fd_{y1}]_g^i + [Fd_{y2}]_g^i,$$

$$\frac{\partial \rho_g e_g}{\partial t} + \frac{\partial u_g(\rho_g e_g + P)}{\partial x} + \frac{\partial v_g(\rho_g e_g + P)}{\partial y} = [Fd_{x1}]_g^i u_{s1} + [Fd_{y1}]_g^i v_{s1} + [Fd_{x2}]_g^i u_{s2} + [Fd_{y2}]_g^i v_{s2};$$

$$\frac{\partial \rho_{s1}}{\partial t} + \frac{\partial \rho_{s1} u_{s1}}{\partial x} + \frac{\partial \rho_{s1} v_{s1}}{\partial y} = 0,$$

$$\frac{\partial \rho_{s1} u_{s1}}{\partial t} + \frac{\partial \rho_{s1} u_{s1}^2}{\partial x} + \frac{\partial \rho_{s1} u_{s1} v_{s1}}{\partial y} = -[Fd_{x1}]_g^i,$$

$$\frac{\partial \rho_{s1} v_{s1}}{\partial t} + \frac{\partial \rho_{s1} u_{s1} v_{s1}}{\partial x} + \frac{\partial \rho_{s1} v_{s1}^2}{\partial y} = -[Fd_{y1}]_g^i,$$

$$\frac{\partial \rho_{s2}}{\partial t} + \frac{\partial \rho_{s2} u_{s2}}{\partial x} + \frac{\partial \rho_{s2} v_{s2}}{\partial y} = 0,$$

$$\frac{\partial \rho_{s2} u_{s2}}{\partial t} + \frac{\partial \rho_{s2} u_{s2}^2}{\partial x} + \frac{\partial \rho_{s2} u_{s2} v_{s2}}{\partial y} = -[Fd_{x2}]_g^i,$$

$$\frac{\partial \rho_{s2} v_{s2}}{\partial t} + \frac{\partial \rho_{s2} u_{s2} v_{s2}}{\partial x} + \frac{\partial \rho_{s2} v_{s2}^2}{\partial y} = -[Fd_{y2}]_g^i.$$

The second family is initially set to zero. When particles of the first family reach the symmetry axis, we apply to this set of equations absorption conditions, while for particles of the second family we apply reflective conditions for the computation of fluxes at the axis of symmetry (Figure 8):

$$\vec{V}_{s1,sym} \cdot \vec{n} = \vec{V}_{s1,\omega_{sym}} \cdot \vec{n}, \qquad \vec{V}_{s1,sym} \cdot \vec{t} = \vec{V}_{s1,\omega_{sym}} \cdot \vec{t}, \qquad \rho_{s1,sym} = \rho_{s1,\omega_{sym}};$$

$$\vec{V}_{s2,sym} \cdot \vec{n} = -\vec{V}_{s1,\omega_{sym}} \cdot \vec{n}, \qquad \vec{V}_{s2,sym} \cdot \vec{t} = \vec{V}_{s1,\omega_{sym}} \cdot \vec{t}, \qquad \rho_{s2,sym} = \rho_{s1,\omega_{sym}}.$$

2.2.3. Coupling of the gas and particle systems. Once the solution of the two homogeneous systems (gas and particles) has been found, the solution of the non-homogeneous system (7), (8) is to be obtained by integration in time over the interaction terms. This means that we have to solve $dU/dt = H$, where H contains the coupling terms. A fourth-order explicit Runge–Kutta procedure has been used. When the source terms are strong, the time step for integration is reduced according to the criterion $\Delta t = \Delta t_{CFL}/m$, with $m = \text{int}(|\vec{V}_g - \vec{V}_s|/D)$, and integration of the previous set of ODEs is performed until the number of iterations reaches m. The value used for D in many applications is $D = 10\ \text{m s}^{-1}$.

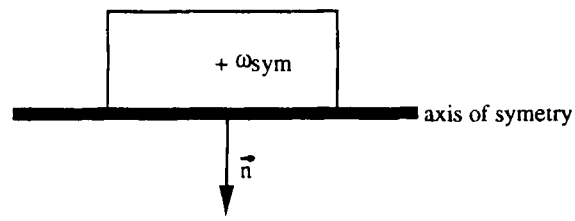

Figure 8. Mesh element close to the axis of symmetry

3. RESULTS

Before presenting results illustrating the capabilities of the method, we have to validate it. The validation of a two-phase numerical code is difficult, because experiments in two dimensions are rather rare; two-phase shock tube experiments give one-dimensional results and other experiments are generally three-dimensional. As an alternative we propose to perform the validation of the present method by making a comparison with an existing scheme. When the geometry of the physical problem is not too complex, a central scheme such as the MacCormack[6] finite difference method can be used to solve systems (7) and (8). Two-phase computations in nozzle flows have already been achieved with this scheme.[25,26] We compare here results obtained by this central scheme with those obtained by our upwind scheme. The MacCormack scheme is widely used, so no particular comment is given here. The equations are solved in a Cartesian computational domain after mathematical transformation. In addition, a second-order damping term is added to avoid non-linear instabilities. The physical problem chosen as a test case is a difficult one, because the two-phase nature of the flow results from the injection of droplets into a gaseous inviscid stream in a nozzle. When the injection of particles is considered, two kind of flows are encountered: a one-phase flow upstream of the injection and a two-phase flow downstream. Some difficulties appear generally[26] at the boundary between the single-phase and the two-phase flow. Droplets are injected through two symmetrical injectors (with respect to the axis of the nozzle). To treat the problem, boundary conditions have to be set.

For the gas flow

(i) Inlet: reservoir conditions ($P = 4{\cdot}5$ atm, $T = 900$ K).
(ii) Outlet: reservoir conditions ($P = 1$ atm, $T = 300$ K).
(iii) Duct walls: symmetry conditions (reflection).

For the particles

(i) Nozzle inlet: no particles ($\rho_s = 0$).
(ii) Nozzle outlet: absorption (extrapolation) conditions.
(iii) Nozzle walls: the wall is assumed impervious and particles are assumed not to adhere nor to reflect. Thus they are sliding along the wall. This constraint may be satisfied by imposing the simple conditions $\rho_{s,\,\mathrm{wall}} = \rho_{s,\,\omega_{\mathrm{wall}}}$, $u_{s,\,\mathrm{wall}} = -u_{s,\,\omega_{\mathrm{wall}}}$ and $v_{s,\,\mathrm{wall}} = v_{s,\,\omega_{\mathrm{wall}}}$ when computing the wall fluxes. The reflection condition applied to the particle equation system reduces to a sliding condition when applying the conservation law on the control volume at the wall. For the finite difference scheme the upwind Warming and Beam[27] scheme is used.
(iv) Injection: $\rho_s = 6\ \mathrm{kg\ m^{-3}}$ with a real density of the injected particles of $1000\ \mathrm{kg\ m^{-3}}$, corresponding to a void fraction $\alpha = 0{\cdot}994$. In addition, the injection velocity is $v_s = 18\ \mathrm{m\ s^{-1}}$ ($u_s = 0$) and the particle diameter is set to 50 μm.

Initial conditions

The gas is at rest under standard atmospheric conditions: initially the nozzle does not contain any particles ($\rho_s = 0$).

Closure relations

(i) Equation of state: the gas is assumed perfect, i.e. $P = (\gamma - 1)\,\rho\, e$, with $\gamma = 1{\cdot}4$. Real gas effects could readily be taken into account by using van der Waals' equation, for

example, since exact solutions to the Riemann problem for a real gas may be computed using the procedure developed by Larini *et al.*[28]

(ii) Drag force:

$$[\vec{F}_d]_g^i = 6\,\pi r_p\,\mu\,(\vec{U}_s - \vec{U}_g)N_p f_d, \quad \text{with } f_d = 0{\cdot}01833Re \text{ (drag coefficient)},$$

where r_p is the particle radius and N_p is the number of particles per unit volume (of the order of 10^{11} particles m^{-3}).

The results presented relate to the steady state obtained after a run of 700 cycles with a time step of 0·7 CFL. The contours of ρ_S are shown in Plate 1. The results are quite comparable. The two jets of droplets from the two injectors have met each other. One can notice a slight difference between the two schemes with respect to the size of the jet at the exit: it is larger with the MacCormack scheme than with the upwind scheme. This is clearly seen in Figure 9, where a cross-section of the particle density in the divergent part of the nozzle is plotted. This difference is due to the second-order damping term necessary for the MacCormack scheme and its poor handling of contact-discontinuity-type waves. Actually, the boundary between the one-phase and the two-phase flow characterized by the contour of the particle jet is a contact-discontinuity-type wave. All other details about the comparison of the two schemes can be found in Reference 29.

The next problem uses the same initial conditions and closure relations as previously. The gas boundary conditions are identical. The injection boundary conditions are harder: $\rho_s = 50\ kg\ m^{-3}$, corresponding to a void fraction $\alpha = 0{\cdot}95$, the injection velocity is equal to $70\ m\ s^{-1}$ and the particle diameter is set to 10 μm. The main difficulty remains in the geometry. From a reservoir a gas outflow is generated into a nozzle followed by a bend; in a certain section of the nozzle particles are injected (Figure 10).

The following results present the velocity fields for the gas and particles as well as the density distributions at steady state. The duration of the simulation was about 5 min CPU time on an

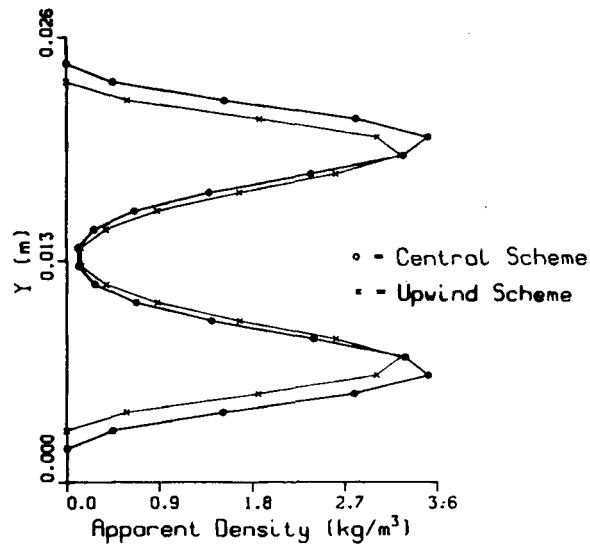

Figure 9. Cross-section of particle density at steady state in diverging part of nozzle

Central scheme:

Upwind scheme:

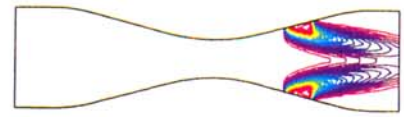

Plate 1. Particle density contours at steady state

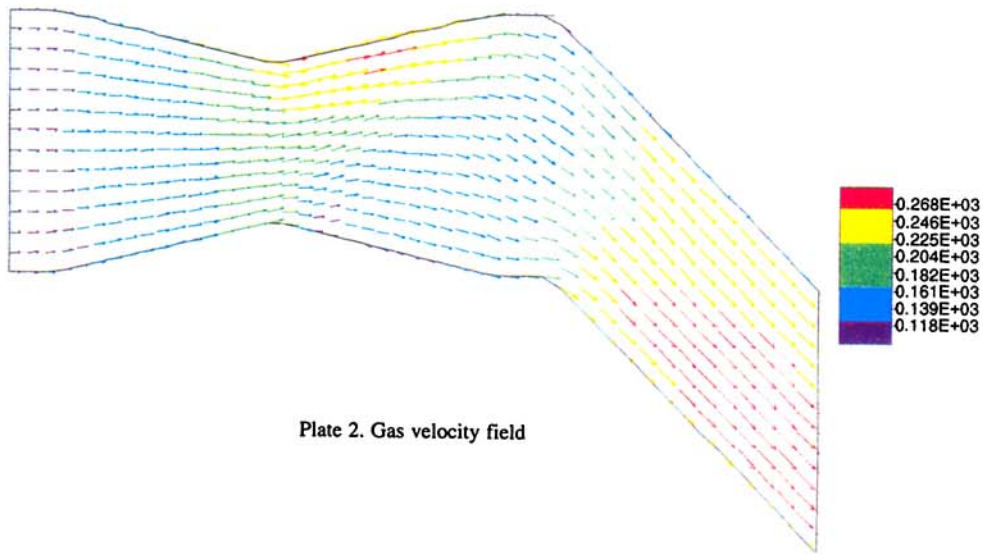

Plate 2. Gas velocity field

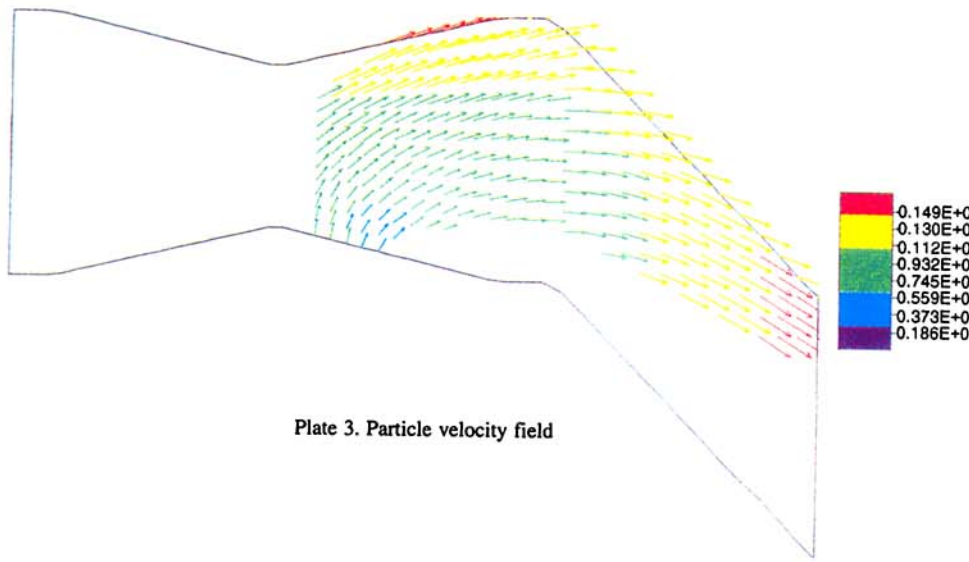

Plate 3. Particle velocity field

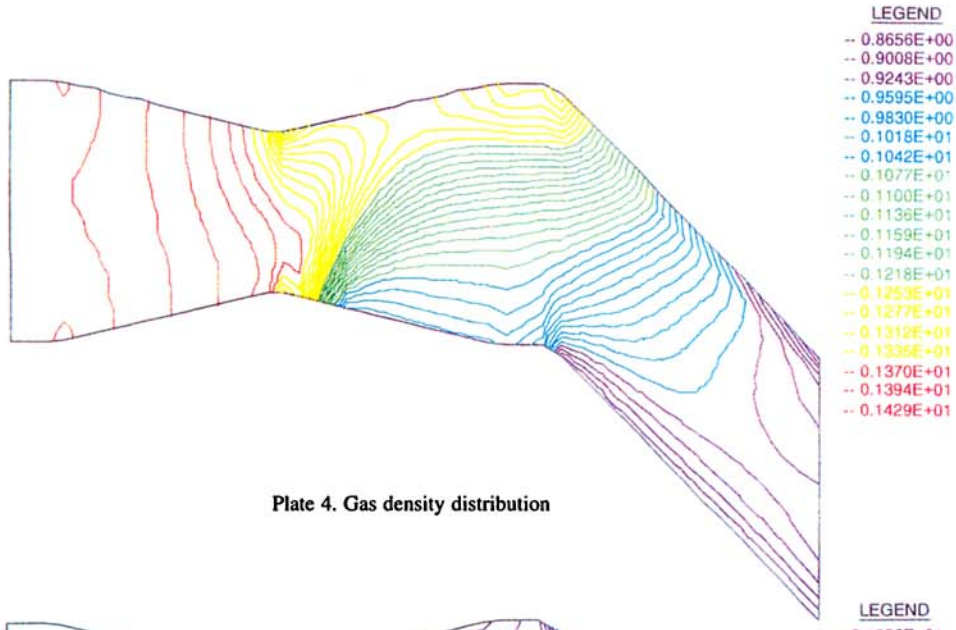

Plate 4. Gas density distribution

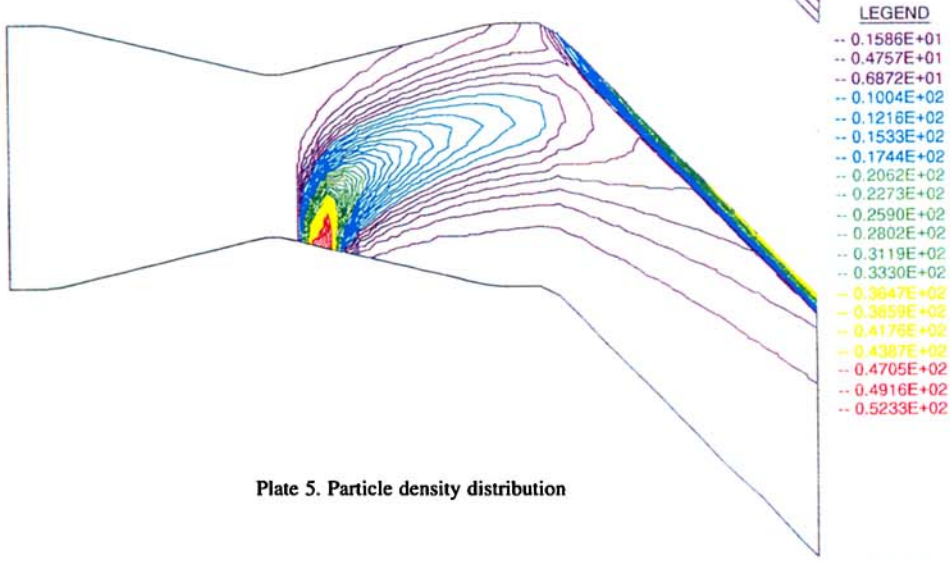

Plate 5. Particle density distribution

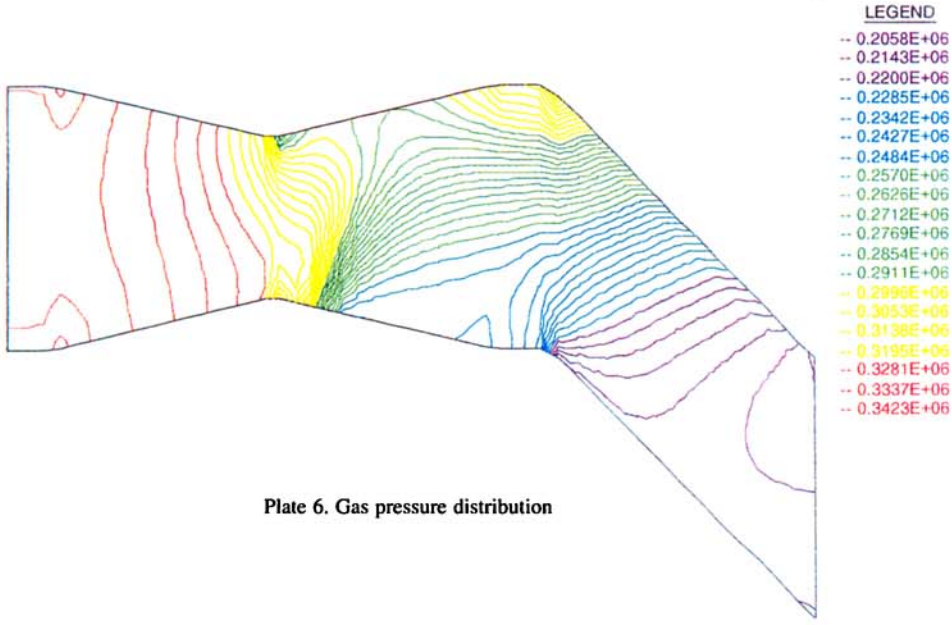

Plate 6. Gas pressure distribution

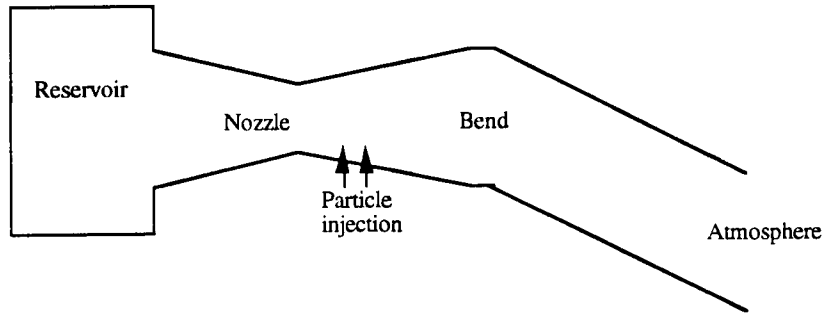

Figure 10. As Figure 8 but for a 15 km wide seamount

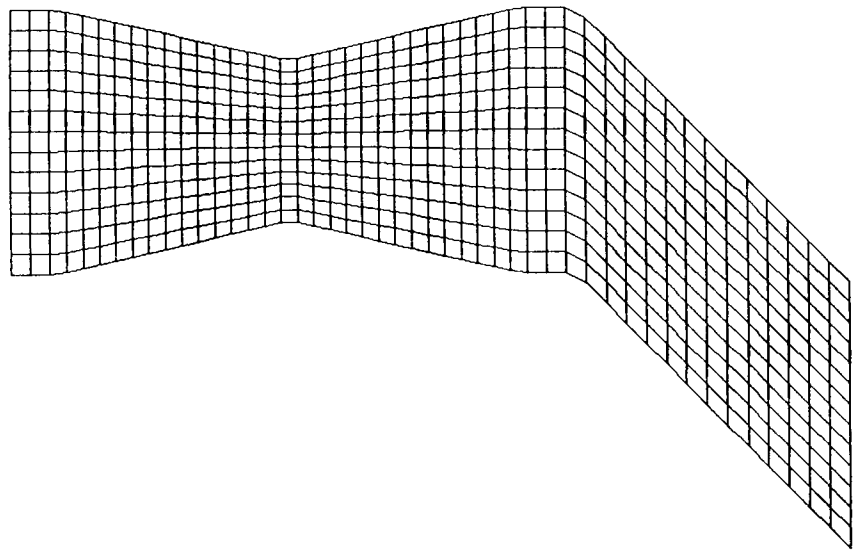

Figure 11. Grid configuration

IBM 3090 using the fast and exact Riemann solver of Gottlieb and Groth[30] for the gas phase. Plates 2–6 and Figure 11 show the gas velocity field, the particle velocity field, the gas density distribution, the particle density distribution, the gas pressure distribution and the grid configuration respectively.

The high resolution of the particle fronts is emphasized in Plates 3 and 5: one may notice that in Plate 3 the regions containing particles and those free of them are well resolved; the regions with high particle concentrations are also readily identified.

4. CONCLUSIONS

An efficient numerical method has been developed for the treatment of gas–particle two-phase flows. It is based upon a second-order TVD scheme for the gas, while the particle flow is treated by an upwind method derived from the donor–cell method. The solution to the Riemann problem for the equations of the dispersed phase is also developed and linked into the

donor–cell algorithm. Particular care must be taken when particle compressions (as defined above) occur.

Results are presented for a specific problem dealing with the injection of particles into a nozzle where it was necessary to follow the development of particle fronts. Later on we intend to focus our attention on a second-order treatment of the particle flow equations.

APPENDIX: NOMENCLATURE

e	total internal energy
E_{chem}	reaction energy in a combustion process
f_{d}	drag coefficient
F_{d}	drag force
F_1	vector of conservative fluxes along x
F_2	vector of conservative fluxes along y
$\vec{n}$	normal unit vector, pointing outwards from element T_j, for segment $\delta T_j \cap \delta T_{jk}$
n_1, n_2	components of vector $\vec{n}$
N_{p}	number of particles per unit volume
P	pressure
Q	convective heat flux
Re	Reynolds number
R_{p}	intergranular stress tensor
S_j	area of element T_j
u, v	barycentric velocity components in x- and y-direction respectively
U	vector of conservative parameters
W	solution of exact Riemann problem

Greek letters

α	volume fraction
δT_j	boundary of element T_j
$\delta T_j \cap \delta T_{jk}$	interface between element T_j and element T_{jk}
d_j^n	slope of conservative variables along x at time n for element T_j
δ_j^n	slope of conservative variables along y at time n for element T_j
Γ	mass transfer flux
Γ_{EC}	kinetic energy flux due to mass transfer
Γ_{V}	momentum flux due to mass transfer
μ_{c}	dynamic compaction viscosity
ρ	specific mass
ω_j	centre of gravity of element T_j

Subscripts

l	left state
g	gas phase
r	right state
s	dispersed phase

Superscripts

i	interface between gas and dispersed phase
j	identifying index of an element
*	solution state of Riemann problem

REFERENCES

1. G. Hetsroni, *Handbook of Multiphase Systems*, Hemisphere/McGraw-Hill, 1982.
2. M. R. Baer and J. W. Nunziato, 'A two-phase mixture theory for the deflagration-to-detonation transition (DDT) in reactive granular materials', *Int. J. Multiphase Flow*, **12**, 861–889 (1986).
3. R. Saurel, M. Larini and J.-C. Loraud, 'Ignition and growth of a detonation by a high-energy plasma', *Int. J. Shock Waves*, **2**, 19–29 (1992).
4. R. Saurel, M. Larini and J.-C. Loraud, 'Numerical modelling of deflagration transition produced by laser impact on granular explosive', *J. Comput. Fluid Dyn.*, **1**, 155–174 (1992).
5. P. Embid and M. Baer, 'Mathematical analysis of a two-phase continuum mixture theory', *Continuum Mech. Thermodyn.*, **4**, 279–312 (1992).
6. R. W. MacCormack, 'The effect of viscosity in hypervelocity impact cratering', *AIAA Paper 69-354*, 1969.
7. B. van Leer, 'Towards the ultimate conservative scheme V. A second-order sequel to Godunov's method', *J. Comput. Phys.*, **32**, 101–136 (1979).
8. P. L. Roe, 'Approximate Riemann solvers, parameter vectors and difference schemes', *J. Comput. Phys.*, **43**, 357–372 (1981).
9. D. L. Book, J. P. Boris and K. Haim, 'Flux-corrected transport II: generalisation of the method', *J. Comput. Phys.*, **18**, 243–283 (1975).
10. E. F. Toro, 'Riemann problem-based techniques for computing reactive two-phase flows', *CoA Rep. 8815*, Aerodynamics, Cranfield Institute of Technology, 1988.
11. S. K. Godunov, 'A finite-difference method for the numerical computation of discontinuous solutions of the equations of fluid dynamics', *Math. Sb.*, **47**, 357–393 (1959).
12. G. Rudinger, 'Some effects of finite partial volume on the dynamics of gas–particle mixtures', *AIAA J.*, **5**, 1917–1922 (1965).
13. R. Ishii, Y. Umeda and M. Yuhi, 'Numerical analysis of gas–particle two-phase flows', *J. Fluid Mech.*, **203**, 475–515 (1989).
14. M. Olim, O. Igra, M. Mond and G. Ben-Dor, 'A general attenuation law of planar shock waves propagating into dusty gases', *Proc. Symp. on Shock Tubes*, 1987, pp. 684–689.
15. A. S. Levine and B. Otterman, 'Analysis of unsteady supersonic two-phase flows by the particle-in-cell method', *Comput. Fluids*, **3**, 111–123 (1975).
16. H. Miura and I. I. Glass, 'On a dusty-gas shock-tube', *Proc. R. Soc. Lond. A*, **382**, 373–388 (1982).
17. R. Saurel, J.-C. Loraud and M. Larini, 'Optimisation of a pyrotechnic igniter by the release of pyrotechnic particles', *Int. J. Shock Waves*, **1**, 121–133 (1991).
18. F. A. Williams, *Combustion Theory*, Benjamin/Cummings, New York, 1988.
19. P. Kuentzmann, *Aerothermochimie des Suspensions*, Gauthier-Villars, Paris, 1973.
20. M. Sommerfeld, 'Numerical simulation of supersonic two-phase gas–particle flows', *Proc. Symp. on Shock Tubes*, pp. 235–241.
21. J. K. Dukowicz, 'A particle–fluid numerical model for liquid sprays', *J. Comput. Phys.*, **35**, 229–253 (1980).
22. L. Sainsaulieu and P. A. Raviart, 'A non-conservative convection–diffusion system describing spray dynamics', in preparation.
23. A. Forestier, 'Second-order scheme for Euler equations in bidimensional unstructured geometries', *J. Comput. Phys.*, submitted.
24. A. Forestier and P. Le Floch, 'Multivalued solutions to some non-linear and non-strictly hyperbolic systems', *Jpn. Ind. Appl. Math.*, **9**, 1–23 (1992).
25. I. S. Chang, 'One and two-phase nozzle flows', *AIAA J.*, **18**, 1455–1461 (1980).
26. E. Daniel, M. Larini, J.-C. Loraud and B. Porterie, 'A numerical simulation of injection of droplets in a compressible flow', *AIAA Paper 92-929*, 1992.
27. R. F. Warming and R. M. Beam, 'Upwind second order schemes and applications in aerodynamic flows', *AIAA J.*, **14**, (1976).
28. M. Larini, R. Saurel and J.-C. Loraud, 'An exact Riemann solver for detonation products', *Int. J. Shock Waves*, **2**, 225–236 (1992).
29. E. Daniel, R. Saurel, M. Larini and J.-C. Loraud, 'A comparison between centered and upwind schemes for two-phase compressible flows', *AIAA Paper 93-2346*, 1993.
30. J. J. Gottlieb and C. P. T. Groth, 'Assessment of Riemann solvers for unsteady one-dimensional inviscid flows of perfect gases', *J. Comput. Phys.*, **78**, 437–458 (1988).